# Primary Charge−Separation Rate at 5 K in Isolated Photosystem II Reaction Centers Containing Five and Six Chlorophyll a Molecules

**ARTICLE** *in* THE JOURNAL OF PHYSICAL CHEMISTRY B · JANUARY 2002

Impact Factor: 3.3 · DOI: 10.1021/jp021787d



**7 AUTHORS**, INCLUDING:

Ryszard Jankowiak
Kansas State University
**194** PUBLICATIONS **4,778** CITATIONS
SEE PROFILE

Valter Zazubovich
Concordia University Montreal
**43** PUBLICATIONS **714** CITATIONS
SEE PROFILE

# Primary Charge-Separation Rate at 5 K in Isolated Photosystem II Reaction Centers Containing Five and Six Chlorophyll *a* Molecules

**R. Jankowiak,[†] M. Rätsep,[‡] J. Hayes,[†] V. Zazubovich,[†] R. Picorel,[§,||] M. Seibert,[||] and G. J. Small*[,†]**

*Ames Laboratory, USDOE, and Department of Chemistry, Iowa State University, Ames, Iowa 50011, Institute of Physics, University of Tartu, 51014 Tartu, Estonia, E. E. Aula Dei (CSIC), Apdo. 202, 50080 Zaragoza, Spain, and National Renewable Energy Laboratory, Golden, Colorado 80401*

*Received: August 6, 2002; In Final Form: November 12, 2002*

Although the primary charge-separation rate in the photosystem II (PSII) reaction center (RC) has been the subject of many time- and frequency-domain experiments, its value is still an unsettled issue, especially at or near room temperature. As a first step toward understanding its temperature dependence, it is important to have a reliable value for the rate at liquid helium temperatures. Presented are results from triplet bottleneck hole-burning (TBHB) experiments at 5.0 K on RCs isolated from spinach that contain either six or five chlorophyll *a* (Chl) molecules per two pheophytin (Pheo) molecules (referred to as RC-6 and RC-5). RC-5 possesses only one of the two peripheral Chls of the RC. The triplet state that serves as the population bottleneck is formed by charge recombination of the radical ion pair $P680^{+}\,Pheo_1^{-}$, where P680 is the primary electron donor and $Pheo_1$ is the acceptor on the active ($D_1$) branch. In the TBHB experiments, the laser burn intensity was varied over 2 orders of magnitude to assess the contribution from fluence broadening to the width of the zero-phonon hole (ZPH) burned into the P680 absorption band. The widths of the ZPH were also corrected for interference from a weak and sharp hole contribution from a state(s) that is unlikely to be involved in efficient charge-separation. The corrected ZPH widths for RC-5 and RC-6 were the same ($2.3 \pm 0.2$ cm$^{-1}$) and correspond to a charge-separation rate of $(4.6 \pm 0.4$ ps$)^{-1}$, in good agreement with a value recently measured for RC-6 by femtosecond pump−probe spectroscopy at 7 K (Greenfield, S. R.; Seibert, M.; Wasielewski, M. R. *J. Phys. Chem. B* **1999**, *103*, 8364). It appears that the removal of a peripheral Chl does not lead to structural changes in the core region of the RC that affect primary charge separation.

## 1. Introduction

Understanding the $Q_y(S_1)$ excitonic structure, excitation energy transfer, and primary charge-separation processes of the isolated $D_1/D_2$-cyt $b_{559}$ photosystem II (PSII) reaction center (RC) has proven to be a challenging problem, as recently reviewed in ref 1. To a large extent, this is the result of the severe spectral congestion of the $Q_y$ absorption spectrum due to the six chlorophyll *a* (Chl) and two pheophytin *a* (Pheo) molecules of the RC. This composition was confirmed by the recently determined 3.8-Å resolution X-ray structure by Zouni et al.,[2] which is quite similar to the model structure of Svensson et al.[3] Hereafter, we will refer to this RC as RC-6. Two of the six Chl molecules are peripheral and bound by histidines of the $D_1$ and $D_2$ polypeptides, which are analogous to the L and M RC polypeptides of purple bacteria. The peripheral Chls are sometimes referred to as $Chl_Z$ molecules.[4,5] A view of the other four Chls and two Pheos (core chlorins) is shown in Figure 1. The structural arrangement is similar to that of the four bacteriochlorophyll (BChl) and two bacteriopheophytin (BPheo) molecules of the bacterial RC, which does not possess peripheral BChl molecules.[6−8] The $P_1$ and $P_2$ Chl molecules are analogous to $P_L$ and $P_M$, the special BChl pair of the bacterial RC whose lowest excited level ($P_-$) is the primary electron-donor state.

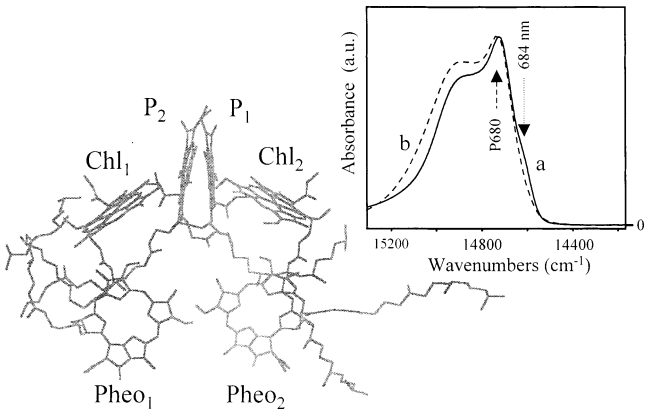


**Figure 1.** View of the structural arrangement of the core cofactors (chlorins) of the PSII RC based on the structural model of Svensson et al.[3] Subscripts 1 and 2 indicate that the cofactor is bound to the $D_1$ or $D_2$ polypeptides. (The $P_1$ and $P_2$ Chl molecules have not been inadvertently interchanged; see ref 10 for a different view of the structure.) The inset shows the 5.0 K $Q_y$ absorption spectra of RC-5 (a) and RC-6 (b). The primary electron donor, P680, is a major contributor to the most intense band at ∼680 nm.

The X-ray structure of Zouni et al. indicates an important difference between the two RCs, which is that the Mg···Mg distance between $P_1$ and $P_2$ is 10 Å, which is 2.4 Å longer than the distance between $P_L$ and $P_M$. Thus, the excitonic coupling between $P_1$ and $P_2$ would be expected to be considerably weaker than that between $P_L$ and $P_M$.[9−11] However, a recent refinement

* Corresponding author. E-mail: gsmall@ameslab.gov.
[†] Iowa State University.
[‡] University of Tartu.
[§] E. E. Aula Dei (CSIC).
[||] National Renewable Energy Laboratory.

10.1021/jp021787d CCC: $25.00 
Published on Web 02/08/2003

of the X-ray structure has led to a $P_1-P_2$ distance of 8.6 Å.[12] This distance may still be too large for significant electron-exchange coupling between $P_1$ and $P_2$, which is known to be important for $P_L$ and $P_M$, as reviewed in ref 13.

The 4 K $Q_y$ absorption spectrum of RC-6 is shown in the inset of Figure 1. Also shown is the absorption spectrum of RC-5, a preparation in which one of the two peripheral Chls has been removed.[14] The spectra span a range of only ~700 $cm^{-1}$, which is much smaller than the ~2500 $cm^{-1}$ range for the RC of the purple bacterium *Rhodobacter sphaeroides*.[15] In the latter spectrum, the primary electron-donor absorption band (P870) due to $P_L$ and $P_M$ is well resolved from higher absorption bands due to the accessory BChl *a* molecules and the two BPheo *a* molecules. As a result, P870* (* indicating the lowest excited state of the special pair) is highly localized on $P_L$ and $P_M$, which are strongly coupled with an interaction energy of ~700 $cm^{-1}$ at 4 K.[13] (This coupling is much larger than other pairwise couplings in the bacterial RC.) The contributions from electrostatics and electron exchange to this coupling are roughly equal. The absorption band in the PS II RC that is analogous to the P870 band of the bacterial RC is P680 (Figure 1). Calculations for the core chlorins of the PSII RC have shown that[9-11,16] the electrostatic coupling between $P_1$ and $P_2$ is the largest (~150 $cm^{-1}$) of all pairwise electrostatic couplings, although only by about a factor of 2−3 larger in magnitude than the $Pheo_1-Chl_1$, $P_2-Chl_1$, $P_1-Chl_1$, and $P_2-Chl_2$ couplings.[17] This, together with the narrow range spanned by the $Q_y$ absorption spectrum, suggests that the $Q_y$ states should be significantly delocalized and, in particular, that there may not be a P680* state that is highly localized on $P_1$ and $P_2$, unlike the situation for $P_L$ and $P_M$. The calculations in ref 10 were based on the RC structure of Svensson et al.[3] and the X-ray structure of Zouni et al.[2] (Because the resolution of the X-ray structure is too low to provide the orientations of the $Q_y$ transitions, orientations that most closely resemble those in the structure of Svensson et al. were used.) The calculations took into account diagonal energy disorder due to structural heterogeneity. The results obtained for the structures of Svensson et al. and Zouni et al. were similar. In particular, $P_1$ and $P_2$ were found, on average, to make the largest contribution (~30% each) to P680*, but the contributions from $Chl_1$ and $Pheo_1$ were significant. It was shown that the composition can vary significantly from complex to complex, a consequence of the site excitation distribution functions of the chlorins being uncorrelated. Thus, unlike P870*, P680* appears to be not so well defined.[18] This suggests that the kinetics for primary charge separation in the PSII RC might be dispersive (nonsingle exponential). The photon echo data of Prokorenko and Holzwarth obtained for RC-6 at 1.33 K indicate that this may be the case.[19] It should be kept in mind, however, that if the exciton−phonon coupling is sufficiently strong it can lead to a coherence loss of the initially excited P680* state on a time scale shorter than that of charge separation.[20,21] This could lead to a redistribution of the electronic excitation between the core chlorins prior to charge separation.

Concerning the primary charge-separation rate of the isolated PSII RC, its value still remains an unsettled issue, especially at temperatures near room temperature. Several femtosecond pump−probe experiments at those temperatures led to the conclusion that the rate is ~$(3\ ps)^{-1}$;[22-25] another led to a value of $(8\ ps)^{-1}$, [26] whereas others led to a value of $(21\ ps)^{-1}$.[27] A value of $(0.4)\ ps^{-1}$ was reported for $T = 240$ K.[28] It is to be appreciated that determination of the charge-separation rate at room temperature is not straightforward because the $Q_y$ absorption spectrum is structureless and because excitation energy transfer processes (both downward and thermally assisted) occur on a subpicosecond and longer time scales[1,16,27] (i.e., on the same time scale as charge separation). At liquid helium temperatures, the situation is somewhat simpler since the $Q_y$ absorption spectrum is structured with a pronounced P680 band and thermally assisted energy-transfer processes do not occur. Both triplet bottleneck hole-burning (TBHB)[29,30] and time-domain pump−probe experiments[28,31,32] led to a rate of ~$(2\ ps)^{-1}$ at liquid helium temperatures. More recently, the 7 K pump−probe experiments by Greenfield et al.[33] resulted in a value of $(5 \pm 1\ ps)^{-1}$, whereas the 1.33 K photon echo data of Prokorenko and Holzwarth led to a rate of $(2-5\ ps)^{-1}$, although the nonsingle exponential echo decay curves suggest that primary charge separation in some RCs may occur with considerably slower rates.[19] All of the above experiments were performed on RC-6-type samples from higher plants such as spinach.

Understanding the temperature dependence of the primary charge-separation rate of the PSII RC is a nontrivial problem because of spectral congestion of the $Q_y$ states because they are significantly delocalized over three to four core chlorins[10,16,34] and because the loss of coherence of the initially excited P680* state due to exciton−phonon coupling is strongly temperature-dependent. A first step toward the solution of this problem is to understand the exciton-level structure, excitation energy transfer, and primary charge-separation processes of the isolated PSII RC at liquid helium temperatures. To this end, we report on the first measurements of the primary charge-separation rate at 5.0 K for RC-5 and compare that rate with the rate for RC-6. The rates were determined by TBHB spectroscopy (also referred to as triplet−singlet spectroscopy) with the triplet state formed by charge recombination of the radical ion pair $P680^+ Pheo_1^-$.[29,35] Unlike in the early TBHB experiments,[29,35] the contribution of burn fluence broadening[36,37] to the zero-phonon hole (ZPH) width was investigated by varying the laser burn intensity over 2 orders of magnitude. In the absence of fluence broadening, the width of the ZPH provides the primary charge-separation rate. Simulations of fluence broadening, which is due to complexes whose P680 zero-phonon line is off-resonance with the laser frequency and absorb via their Lorentzian wings, were performed using the theory of hole spectra given in ref 38. In addition to the observation of fluence broadening, a weak and very narrow contribution to the ZPH was detected that may be due to the 684-nm absorbing Chl whose absorption is shown in Figure 1. Taking this weak contribution and fluence broadening into account led to the same primary charge-separation rate for both RC-5 and RC-6, $(4.6 \pm 0.4\ ps)^{-1}$. Thus, the removal of one of the two peripheral Chls does not lead to structural changes in the core region of the RC that affect the rate.

## 2. Experimental Section

The PSII RC-6 complex was isolated from market spinach following the procedure in ref 26. Pigment content analysis using the spectroscopic method in refs 39 and 40 resulted in 6.0 ± 0.3 Chl *a* per 2 Pheo *a*. The PSII RC-5 complex was prepared and purified according to ref 14 and contained 5.3 ± 0.3 Chl *a* per 2 Pheo *a*. The 4.2 K $Q_y$ absorption spectra of RC-5 and RC-6 shown in Figure 1 are similar to those in refs 14 and 41 for RCs containing ~5 and ~6 Chl *a* molecules. Following the final isolation step, samples were kept frozen at −80 °C until used. To ensure good glass formation, glycerol (66 vol %) was added to the samples just prior to cooling to 5 K in a Janis 8-DT Super Vari-temp liquid helium optical cryostat. Temper-

ature was controlled and measured using a Lakeshore model 330 controller.

The procedure used to reduce the Pheo active in primary charge separation ($Pheo_1$) was as follows: sodium dithionite (8 mg/mL) was added to the glass-forming solution containing RC-5 (4 °C) in an oxygen-free helium atmosphere and in the dark, and the sample immediately cooled to 4 K. The sample was then illuminated with light from a 50-W tungsten−halogen lamp filtered by a 10-cm water-containing cell. The extent of $Pheo_1$ reduction was monitored using the bleach in absorption near 680 nm.[42−45] An illumination time of ∼1 h resulted in complete reduction. Shorter times were used to prepare partially "closed" RCs.

The hole-burning setup that was used is described in ref 42. Briefly, preburn and postburn absorption spectra were recorded with a Bruker HR 120 Fourier transform spectrometer at a resolution of 0.5 $cm^{-1}$. A Coherent CR699 dye laser (line width of 0.07 $cm^{-1}$) pumped by a 6-W Coherent Innova Ar ion laser was used for hole burning. The burn intensities ($I_B$) used are given in the figure captions and text. $I_B$ was varied between 2 and 140 $mW/cm^2$ using glass gray filters (Newport Research Corporation) and was measured at the entrance window of the cryostat with an NRC model 1825 C power meter. The burn wavelengths ($\lambda_B$) used were all close to the maximum of the main absorption band at ∼680 nm (Figure 1) and are given in the figure captions. At these wavelengths, both persistent nonphotochemical hole burning (NPHB) and triplet bottleneck hole burning (TBHB) occurs.[29,42] As first pointed out in ref 29, to obtain a "pure" TBHB spectrum, it is necessary first to saturate the persistent NPHB spectrum before beginning the TBHB experiment. The TBHB spectrum is the difference between the absorption spectrum with the laser on and the absorption spectrum with the laser off. It is the width of the zero-phonon hole (ZPH) of the TBHB spectrum that provides the primary charge-separation rate. The protocol then was first to record the saturated NPHB spectrum, then obtain the TBHB spectrum, and finally record again the persistent NPHB spectrum (laser off). It was found that the last spectrum was identical to the first within experimental uncertainty. This indicates that the TBHB spectra that were obtained were minimally interfered with by persistent NPHB. (For the sake of brevity, we do not present NPHB spectra; they are similar in structure to those in ref 42.) For the discussion in section 4, it is important to note that the widths (full width at half-maximum) of the ZPH in the saturated NPHB spectra were close to 2 $cm^{-1}$, a factor of 4 broader than the read resolution of 0.5 $cm^{-1}$. The saturated ZPH depths obtained with a burn fluence of ∼180 $J/cm^2$ were close to 25%. Unless otherwise noted, the percentage depths of ZPHs given were calculated using $(\Delta A/A) \times 100\%$, where $\Delta A$ is the difference between the absorbance at $\lambda_B$ before burning and the absorbance after burning and $A$ is the absorbance at $\lambda_B$ prior to any burning. (The $A = 0$ baseline used is indicated in the inset of Figure 1.) To assess the contribution from fluence broadening to the width of the triplet bottleneck ZPH, it is necessary to take into account absorption that does not lead to primary charge separation; see section 4.

## 3. Results

The 4.2 K absorption spectra of RC-5 and RC-6 in the $Q_y$ region shown in the inset of Figure 1 are similar to reported spectra of preparations containing ∼5 and ∼6 Chl *a* molecules per RC.[14,41,42] The most intense band at 680 nm (14 706 $cm^{-1}$) is mainly due to P680, the primary electron donor in the isolated RC. Clearly visible in the RC-5 spectrum is a shoulder at ∼684 nm (see arrow). The nature of the 684-nm band (state) continues to be controversial, as reviewed in refs 1 and 42. Although not obvious in the RC-6 spectrum, the 684-nm absorbing Chl *a* exists in RC-6.[41] In that work, persistent (nonphotochemical) ZPH action spectroscopy[46] was used to determine the site-excitation distribution function (SDF) of the 684-nm transition. The width (fwhm) of the SDF, which arises from structural heterogeneity, is ∼140 $cm^{-1}$. The width for RC-5 is ∼150 $cm^{-1}$.[41] Subtraction of the RC-5 and RC-6 spectra in Figure 1 (with normalization at the maximum of the 680-nm band) revealed a loss of absorption for RC-5 centered at ∼665 nm with a width of ∼280 $cm^{-1}$. The loss is due to the removal of one of the two peripheral Chl *a* molecules.[14] We note that the 684-nm absorbing Chl *a* molecules are easily disrupted[42,44,47] so that the difference in 684-nm Chl *a* content between samples from different isolation and handling procedures can be expected.

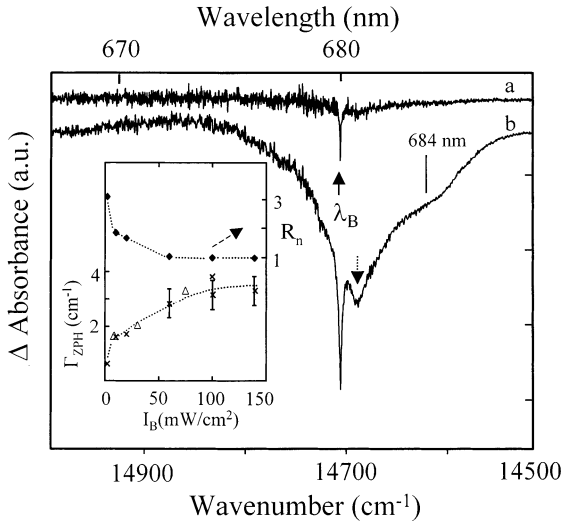


**Figure 2.** Triplet bottleneck hole-burned (TBHB) spectra for RC-5 obtained at 5.0 K with burn intensities ($I_B$) of 2 $mW/cm^2$ (a) and 100 $mW/cm^2$ (b). $\lambda_B$ = 680.0 nm. In both spectra, the sharp ZPH is coincident with the laser burn wavelength $\lambda_B$. The total hole depths are 4% (a) and 23% (b). The feature to the immediate right of the ZPH in spectrum b is the pseudo-PSBH. The left inset shows the ZPH widths vs $I_B$ (bottom) for RC-5 (x) and RC-6 (△). $R_n$ (♦) is the ratio of the total hole depth at $\lambda_B$ relative to that of the pseudo-PSBH normalized to unity at $I_B$ = 100 $mW/cm^2$. $R_n \approx 1$ indicates that both the ZPH and the PSHB are saturated.

In what follows, we present representative triplet bottleneck hole-burned (TBHB) spectra for RC-5 and RC-6 obtained with different burn intensities ($I_B$). As pointed out in section 2, care was taken to ensure that persistent NPHB did not interfere with the TBHB spectra. As an example, Figure 2 shows two TBHB spectra for RC-5 obtained with a burn wavelength ($\lambda_B$) of 680.0 nm, with $I_B$ = 2 $mW/cm^2$ (spectrum a) and $I_B$ = 100 $mW/cm^2$ (spectrum b). The ZPH in both spectra is coincident with $\lambda_B$. The feature to the immediate right of the ZPH in spectrum b (dotted arrow) is the pseudophonon sideband hole (PSBH) due to phonons that peak at ∼17 $cm^{-1}$.[42] Spectrum b is quite similar to those reported earlier for RC-6 samples obtained with high burn intensities.[48] The pseudo-PSBH is not evident in spectrum a because of the low burn intensity used. The depths of the ZPH in spectra a and b, as defined in section 2, are 4 and 23%, respectively. It is evident that the width of the ZPH in spectrum b, which is superimposed on the broad underlying PSBH structure, is considerably broader than the ZPH in spectrum a. The widths are 0.6 and 3.8 $cm^{-1}$, the former being essentially resolution-limited. (See section 2.) The procedure used to

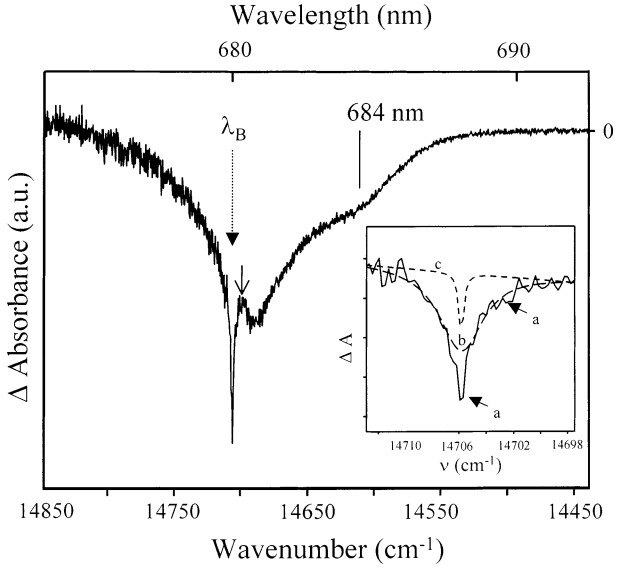


**Figure 3.** TBHB spectrum of RC-5; $I_B = 60$ mW/cm$^2$, 5.0 K, and $\lambda_B = 680.0$ nm. (The depth of the ZPH is 17%.) The inset shows the experimental ZPH (a) that is more sharply tipped than a Lorentzian. It is well fitted by the sum of two Lorentzian ZPHs (b) and (c) with widths of 3.8 cm$^{-1}$ and 0.5 cm$^{-1}$. See text for discussion.

measure hole widths is given below. The 0.6-cm$^{-1}$ ZPH could be equally well fitted with either a Lorentzian or a Gaussian because of a low S/N ratio. The profile of the ZPH with the 3.8-cm$^{-1}$ width was more sharply tipped than a Lorentzian. This effect was observed to become more pronounced as $I_B$ was reduced below 100 mW/cm$^2$ (vide infra). The inset of Figure 2 (bottom curve) shows the dependence of the measured ZPH width ($\Gamma_{ZPH}$, fwhm) on $I_B$. $R_n$ (top curve) is the ratio of the total hole depth at the ZPH peak to its depth at the maximum of the pseudo-PSBH. (See the dashed arrow.) For example, $R_n$ values for curves a and b of Figure 2 (normalized to unity at $I_B = 140$ mW/cm$^2$) are 3.2 and 1.0, respectively. The $\Gamma_{ZPH}$ values indicated by crosses are for the RC-5, whereas the triangles correspond to $\Gamma_{ZPH}$ for RC-6. These results show that $R_n$ reaches a plateau near 50 mW/cm$^2$, whereas the ZPH width continues to increase with increasing burn intensity. A constant value of $R_n$ indicates that both the ZPH and pseudo-PSBH are saturated (i.e., have reached their maximal depths[49]). However, fluence broadening of the ZPH can still occur for burn intensities higher than that required to saturate the ZPH and pseudo-PSBH.[50]

The vertical line in spectrum b of Figure 2 locates a broad low-energy satellite hole at ~684 nm that has been reported in refs 42 and 48. In those works, this hole was assigned to the 684-nm absorbing Chl; see Figure 1. Since the 684-nm band is inhomogeneously broadened, vide supra, it was also suggested that the broad hole in the TBHB spectrum is the result of uncorrelated, downward energy transfer from the state(s) excited at 680 nm, which results in the population of the $Q_y$ singlet state of the 684-nm Chl, after which the population of the triplet state of the 684-nm Chl occurs. Further experiments are required to determine the mechanism of triplet-state formation that can be expected to depend on the nature of the 684-nm absorbing Chl, which, at this time, is not known with certainty.

The RC-5 TBHB spectrum obtained with $\lambda_B = 680.0$ nm and $I_B = 60$ mW/cm$^2$ is shown in Figure 3. The depth at $\lambda_B$ is 17%. The ZPH region is expanded in the inset, noisy profile a. The ZPH profile is distinctly non-Lorentzian but is well fitted by the sum of two Lorentzians, b and c, with widths of 3.8 and 0.5 cm$^{-1}$, respectively. To reduce clutter, the sum spectrum is not shown. An equally good fit was obtained using a Gaussian with a width of 0.5 cm$^{-1}$ for hole c. The depths of the b and c holes (including the ZPH and underlying phonon contribution) are 13 and 4%, respectively, which sum to 17%. Concerning the ZPH component of the hole spectrum shown in the inset, the b and c holes contribute ~60 and ~40%, respectively, on the basis of their peak intensities as measured relative to the chosen baseline of the ZPH profile. For all other TBHB spectra obtained, some of which are shown below, it was also found that the ZPH profile is more sharply tipped than a Lorentzian. It was found that all of the profiles could be fitted with a hole (c) with a constant width of ~0.5 cm$^{-1}$ and a constant depth of ~3−4% plus a second hole (b) whose width and depth depend on the value of $I_B$. Note that the 4% depth and 0.5-cm$^{-1}$ width of hole c in Figure 3 ($I_B = 60$ mW/cm$^2$) are essentially identical to those of the ZPH obtained with $I_B = 2$ mW/cm$^2$ in Figure 2, spectrum a. It appears that the 0.5 cm$^{-1}$-wide ZPH is already saturated with $I_B = 2$ mW/cm$^2$. A possible explanation for this is given in the following section.

The uncertainty in the measured hole widths deserves some discussion. In principle, the most reliable approach is to use the "master equation" for hole spectra[38] to fit the entire hole-burned spectrum, as was done for the TBHB spectra of the primary electron-donor P870 band of *Rhodobacter sphaeroides*[51] and the NPHB spectra of the red-most antenna state of PSI of cyanobacteria.[52,53] Entire means the ZPH plus the broad underlying PSBH structure. Because of the severe spectral congestion in its $Q_y$ absorption region, such an approach is not possible for the PSII RC. Nevertheless, the master equation was used to estimate the error in hole widths determined using the approach in this paper. With reference to the TBHB spectrum in Figure 3, this approach is roughly equivalent to drawing a smooth baseline for the ZPH between the absorbance maximum to the right of the ZPH (see solid arrow) and a point to the left of the ZPH. The master equation requires as input the single site absorption profile (the zero-phonon line plus the phonon wing) and the width of the site excitation distribution function (SDF) associated with structural heterogeneity. Using the results in ref 38 for P680's single site absorption profile and SDF width, it was found that the approach used here introduces an error into the hole widths of ~2%, which is negligible compared to the error associated with the choice of baseline for the ZPH. In the inset of Figure 3, the baseline is defined by that of the short-dashed curve (c) for the ~0.5 cm$^{-1}$-wide hole. By varying the tilt of that baseline (as well as those in other TBHB spectra) within reasonable bounds, an uncertainty of approximately ±10% for hole widths was estimated for $I_B$ values $\lesssim$30 mW/cm$^2$, and an uncertainy of ±15% was estimated for $I_B$ values $\gtrsim$60 mW/cm$^2$.

Figure 4 shows the RC-5 TBHB spectrum obtained with $\lambda_B = 680.0$ nm and $I_B = 10$ mW/ cm$^2$. The depth of the ZPH is 12%, and its measured fwhm is 1.6 cm$^{-1}$. Because of the low burn intensity, the ratio of the peak intensity of the ZPH to that of the pseudo-PSBH is considerably higher than in Figure 3. The letter labeling in the left inset of Figure 4, which shows the ZPH region, is the same as that used in the inset of Figure 3. The sharp (c) and broad (b) hole contributions have widths of 0.5 and 2.3 cm$^{-1}$, respectively. The depth of hole c is ~3%, consistent with it being already saturated with $I_B = 2$ mW/cm$^2$, vide supra. The depth of hole b is 9% (including the phonon contribution). Other spectra for both RC-5 and RC-6 obtained with 7.5 mW/cm$^2$ $\leq I_B \lesssim$ 30 mW/cm$^2$ revealed that the widths of the sharp and broad hole contributions are nearly constant at ~0.5 and ~2.3 cm$^{-1}$. At higher burn intensities, the width of

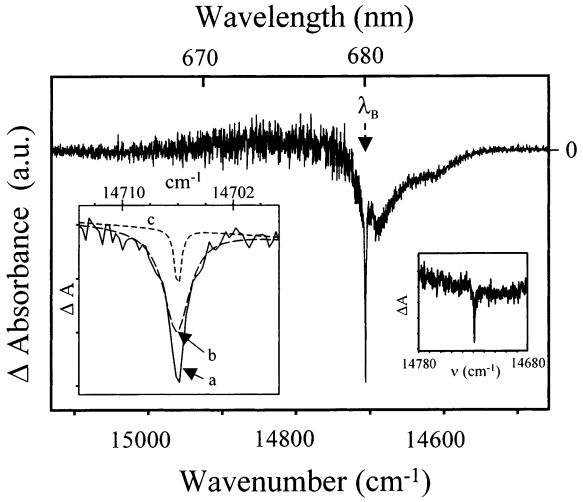


**Figure 4.** TBHB spectrum of RC-5; $I_B = 10$ mW/cm$^2$, $\lambda_B = 680.0$ nm, and 5.0 K. The depth of the ZPH is 12%. See Figure 3 caption for an explanation of the ZPH profiles in the left inset. The widths of holes (c) and (b) are 0.5 and 2.3 cm$^{-1}$, respectively. The right inset shows a ZPH of a closed RC-5 ($\lambda_B = 680.0$ nm) obtained with $I_B = 10$ mW/cm$^2$. Its depth and width are ~4% and ~0.5 cm$^{-1}$, respectively.

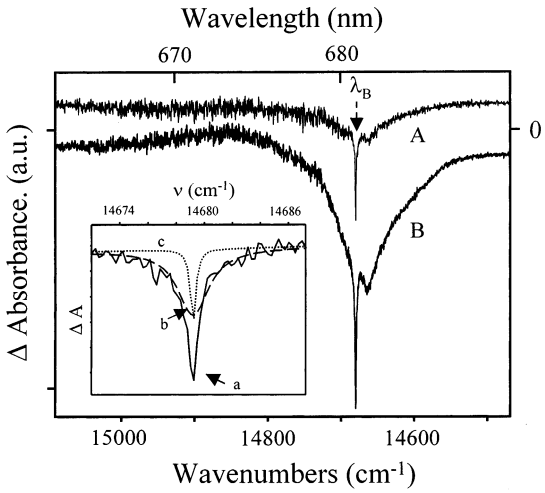


**Figure 5.** TBHB spectrum of RC-6 obtained with $I_B = 7.5$ mW/cm$^2$ (a) and $I_B = 75$ mW/cm$^2$ (b); $\lambda_B = 681.3$ nm, and $T = 5.0$ K. See Figure 3 caption for an explanation of the ZPH profiles in the inset. The widths of holes (c) and (b) are 0.5 and 2.6 cm$^{-1}$, respectively.

the broad hole contribution increased because of fluence broadening; see the following section for a discussion.

Triplet bottleneck hole-burned spectra were also obtained for completely closed RC-5 produced by the reduction of the active $Pheo_1$ by dithionite plus white light illumination. (See section 2.) The TBHB spectra obtained at $\lambda_B = 680.0$ nm with $I_B$ values in the range of 2−20 mW/cm$^2$ were similar to spectrum a of Figure 2; that is, only a resolution-limited ~0.5 cm$^{-1}$ ZPH with a depth of 3−4% was observed. An example for $I_B = 10$ mW/cm$^2$ is shown in the right inset of Figure 4. Since the reduction of $Pheo_1$ prevents the formation of the radical ion pair $P680^+Pheo_1^-$, whose charge recombination leads to triplet formation, it appears that the 0.5-cm$^{-1}$ ZPH is unlikely to be associated with primary charge separation. Spectra obtained with partially closed RC-5 (not shown) exhibited both the ~0.5 cm$^{-1}$ and broader ZPH (b) seen in the insets of Figures 3 and 4. Thus, the broader ZPH results from triplet formation due to charge recombination. To obtain from the width of that ZPH a reliable value for the primary charge-separation rate requires a consideration of fluence broadening; see the following section.

The TBHB spectra for RC-6 obtained with $\lambda_B = 681.3$ nm and $I_B = 7.5$ mW/cm$^2$ (spectrum A) and $I_B = 75$ mW/cm$^2$ (spectrum B) are shown in Figure 5. The respective ZPH depths at $\lambda_B$ are 8 and 18%. The corresponding ZPH widths are 1.6 and 3.3 cm$^{-1}$. The inset shows that the experimental ZPH (a) for $I_B = 7.5$ mW/cm$^2$ is also well fitted by the sum of a narrow ZPH (c) with a width of 0.5 cm$^{-1}$ and a broader hole (b) with a width of 2.6 cm$^{-1}$. Note that the 2.6-cm$^{-1}$ width is within experimental uncertainty the same as that for the broad hole (b) in the left inset of Figure 4. The ZPH obtained with $I_B = 75$ mW/cm$^2$ was also well fitted by the sum of a narrow and broader holes, with the latter fluence broadened.

## 4. Discussion

An analysis of the TBHB spectra shown above revealed that both the ZPH and pseudo-PSBH (at ~17 cm$^{-1}$ relative to the position of the ZPH; see Figure 2) are essentially saturated at $I_B = 100$ mW/cm$^2$ (i.e., have reached their maximum depths). As mentioned, the ZPH at saturation is expected to be fluence-broadened. Before considering fluence broadening of the broad hole (b) contribution to the ZPH, which is of primary interest, it is appropriate to consider first the contribution of the sharp hole (c) to the ZPH.

**Nature of the ~0.5 cm$^{-1}$-Wide ZPH.** The results presented in the preceding section show that the width of the sharp ZPH is independent of $I_B$ in the range of 2−100 mW/cm$^2$, 0.5 ± 0.1 cm$^{-1}$ (resolution limited). Moreover, its depth (~3−4%) is weakly dependent on $I_B$, an observation that eliminates the possibility that the 0.5-cm$^{-1}$ feature is an artifact due to scattered laser light reaching the detector of the FT spectrometer. That it is an artifact due to a small amount of spontaneous filling[54] of the persistent hole saturated at the beginning of the experiment that occurs during the acquisition of the TBHB spectrum is also very unlikely. Such filling should produce an apparent hole with a width equal to that of the persistent saturated hole, which for all samples was close to 2 cm$^{-1}$. That is, spontaneous filling occurs "uniformly" with no change in hole width.[54] It seems, therefore, that the 0.5-cm$^{-1}$ triplet bottleneck hole is due to a $Q_y$ state(s) that is not involved in primary charge separation and contributes only weakly to absorption at 680 nm. (Recall that the $Pheo_1$ photoreduction experiments show that the triplet state responsible for the 0.5-cm$^{-1}$ hole is not formed by charge recombination of $P680^+Pheo_1^-$.) A plausible candidate for the above state is that associated with the 684-nm absorption band (see Figure 1), which has been extensively studied by hole burning.[41,42] In this case, the spectra in Figures 2−4 indicate that the 684-nm state undergoes intersystem crossing. According to the results in ref 42, the inhomogeneous width of the 684-nm band is ~100 cm$^{-1}$ (4.3 nm), so some absorption at 680 nm can be expected. The 684-nm state (band) also undergoes persistent NPHB. The results of Völker and co-workers [41] show, for both RC-5 and RC-6, that the ZPH width at 5.0 K is 2.4 GHz, which is twice the width of the zero-phonon line (30 GHz = 1 cm$^{-1}$). The latter is a factor of 12 ×narrower that of the read resolution of 0.5 cm$^{-1}$ used here. This would explain why fluence broadening of the 0.5-cm$^{-1}$ hole was not observed in our experiments. We hasten to add that any Chl *a* absorbing near 680 nm with a sufficiently narrow homogeneous line width (ZPL) could contribute to the 0.5-cm$^{-1}$ hole. Although the quality of isolated PSII RC preparations has definitely improved in recent years, the possibility that they contain some dysfunctional/denatured RCs cannot be excluded at this time.

Another more interesting possibility is that because of intrinsic energy disorder due to structural heterogeneity there is a small

subset of RCs whose "P680" is not equipped to undergo rapid charge separation because of the core chlorin composition of the lowest-energy $Q_y$ state, P680*. (See Introduction.) This possibility is suggested by the $Q_y$ excitonic calculations for the core chlorins presented in ref 10 as well as the photon echo data of Prokorenko and Holtzwarth,[19] which indicate that the kinetics of primary charge separation may be highly dispersive. They concluded that the primary charge-separation time varies from RC to RC from ~2 ps to several hundred picoseconds, with the percentage of RCs characterized by long separation times being quite low. We note that the chlorin composition of P680* that is optimum for charge separation is not firmly established. To explain the very weak dependence of the width of the narrow ~0.5 $cm^{-1}$ hole on $I_B$, the homogeneous widths of the ZPL of the "defective" P680s would need to be considerably narrower than the read resolution of 0.5 $cm^{-1}$. (A ZPL width of 0.05 $cm^{-1}$ corresponds to a 100-ps lifetime.)

**Fluence Broadening of the Broad Contribution to the ZPH in Triplet Bottleneck Hole-Burning (TBHB) Spectra.** The left inset of Figure 2 shows that the measured width (fwhm) of the ZPH increases with increasing burn intensity, $I_B$. The x and open-triangle data points are for RC-5 and RC-6, respectively. The error bars correspond to an approximate ±15% uncertainty in the hole widths. The uncertainty for data points obtained with $I_B \lesssim 30$ mW/$cm^2$ is somewhat smaller, approximately ±10%. The leftmost data point for RC-5 corresponds to a ZPH width of 0.5 $cm^{-1}$; see spectrum a of Figure 2. Deconvolution of the ZPH into a sharp and broad component, as described above, revealed that the width of the broad hole is 2.3 ± 0.3 $cm^{-1}$ for 7.5 mW/$cm^2 \le I_B \le$ 20 mW/$cm^2$. Thus, the ±0.3 $cm^{-1}$ uncertainty masks any fluence broadening that might occur in this intensity range. Therefore, we attribute the 2.3-$cm^{-1}$ width to lifetime broadening due to primary charge separation. The charge-separation rate is $(4.6 \pm 0.4 \text{ ps})^{-1}$, as calculated using the standard expression $(\pi c \Gamma_{ZPH})^{-1}$ for the lifetime, where $\Gamma_{ZPH}$ is the width of the ZPH in $cm^{-1}$ and $c$ is the speed of light. The 4.6 ± 0.4 ps lifetime is in good agreement with the value of 5 ± 1 ps determined by Greenfield et al.[33] for RC-6 at 7 K. (The RC-6 samples we studied were from the same batch Greenfield et al. used.) On the basis of photon echo data obtained for RC-6 at 4.2 K, Prokohorenko and Holtzwarth identified a fast decay component of 2−5 ps that they assigned to primary charge separation.[19] It appears, therefore, that in the low-temperature limit the primary charge-separation rate is about $(5 \text{ ps})^{-1}$ for both RC-5 and RC-6. Thus, the removal of one of the two peripheral Chl *a* molecules does not appear to have a significant effect on the rate.

To simulate fluence broadening of the broad hole (b) that contributes to the ZPH in the TBHB spectra, it is necessary to correct its $I_B$-dependent hole depths given earlier for absorption at 680 nm that is not associated with primary charge separation (i.e., formation of $P680^+Pheo_1^-$). A rough estimate of this contribution to the total absorption is 45%. The main contribution is from absorbers (states) that result in persistent NPHB. We recall that the saturated hole depth of the persistent ZPH is 25% due to the zero-phonon absorption line. The Franck−Condon factor for that line is $\exp(-S)$, where $S$ is the Huang−Rhys factor for coupling to phonons at ~17 $cm^{-1}$. The associated contribution from phononic transitions to absorption at 680 nm is $1 - \exp(-S)$. To be conservative, we set $S = 0.7$, which is at the low end of $S$ factors observed for the $Q_y$ states of photosynthetic complexes.[41] This increases the percentage absorption to ~40%. We note that we were never able to burn persistent nonphotochemical holes in the special pair (P870) absorption band of the RC of *Rb. sphaeroides* (unpublished results). This is understandable since the primary charge-separation rate at 4.2 K is $(1 \text{ ps})^{-1}$,[51] whereas the average rate constant for the most efficient NPHB system yet discovered, Al-phthalocyanine tetrasulfonate in hyperquenched glassy water,[55] is only $(\sim 0.1\ \mu s)^{-1}$. Thus, in general, NPHB is not expected to compete with photochemical hole burning because of primary charge separation that occurs on a picosecond time scale. Finally, an additional 5% is included because of the absorption of the second-lowest-energy $Q_y$ state of the core chlorins (P680* being the lowest). This percentage is based on the results of excitonic calculations in ref 10. The multiplicative correction factor for the hole depth is (1/0.55) = 1.8. For example, the depth of the broad hole (b) in the inset of Figure 4 ($I_B$ = 10 mW/ $cm^2$) is 9%; the corrected value is 16%. The width of hole (b) is 2.3 ± 0.4 $cm^{-1}$. The corrected depth of hole b in Figure 3 ($I_B$ = 60 mW/$cm^2$) is 23% with a width of 3.8 ± 0.6 $cm^{-1}$. Simulations of fluence broadening were carried out for the P680 absorption band using the master equation for hole spectra given in ref 38. This equation has been successfully applied to several photosynthetic complexes, including PS I[52,53] and the bacterial RC[51], and is reviewed in ref 56. The single site absorption spectrum of P680 that was used was defined by $S = 1.6$, $\omega_m = 20$ $cm^{-1}$, $\Gamma_L = 12.5$ $cm^{-1}$, $\Gamma_G = 7.5$ $cm^{-1}$, and $\gamma = 1.15$ $cm^{-1}$, where $S$ is the Huang−Rhys factor for a one-phonon profile peaked at $\omega_m = 20$ $cm^{-1}$. This profile was modeled by a Gaussian with a half-width of $\Gamma_G = 7.5$ $cm^{-1}$ on its low-energy side and a Lorentzian with a half-width of $\Gamma_L$ = 12.5 $cm^{-1}$ on its high-energy side. $\gamma$ is the homogeneous width of the zero-phonon line that results in a ZPH width of 2 × 1.15 $cm^{-1}$ = 2.3 $cm^{-1}$ in the zero-burn fluence limit. The inhomogeneous width of P680's site excitation distribution function (SDF) was set equal to 120 $cm^{-1}$, and $\lambda_B$ was located at the maximum of the SDF. The above parameter values are similar to those given in ref 57. The calculated fluence broadening for the first of the above two holes with a depth of 16% is 0.2 $cm^{-1}$, which would not be expected to be detectable given the ±0.2 $cm^{-1}$ uncertainty in the measured hole width. The fluence broadening for the 23% hole is 0.5 $cm^{-1}$. Thus, the predicated width of 2.8 $cm^{-1}$ is narrower than the measured width of 3.8 $cm^{-1}$. However, the uncertainty in the latter width is large, ±0.6 $cm^{-1}$, so the actual discrepancy could be as small as 0.4 $cm^{-1}$. We also performed calculations on a number of model systems, the results of which were also consistent with fluence broadening being essentially negligible for hole depths ≲10%.

**Acknowledgment.** Research at the Ames Laboratory was supported by the Division of Chemical Sciences, Office of Energy Sciences, U.S. Department of Energy. Ames Laboratory is operated for the USDOE by Iowa State University under Contract W-7405-Eng-82. M.S. acknowledges support by the Division of Energy Biosciences (USDOE), and R.P., support by MCYT (Grant PB98-1632).

## References and Notes

(1) Dekker, J. P.; van Grondelle, R. *Photosynth. Res.* **2000**, *63*, 195.
(2) Zouni, A.; Witt, H. T.; Kern, J.; Fromme, P.; Krauss, N.; Saenger, W.; Orth, P. *Nature (London)* **2001**, *409*, 739.
(3) Svensson, B.; Etchebest, C.; Tuffery, P.; van Kan, P.; Smith, J.; Styring, S. *Biochemistry* **1996**, *35*, 14486.
(4) Xiong, J.; Subramanian, S.; Govindjee. *Photosynth. Res.* **1998**, *56*, 229.
(5) Koulougliotis, D.; Innes, J. B.; Brudvig, G. W. *Biochemistry* **1984**, *33*, 11814.
(6) Deisenhofer, J.; Epp, O.; Miki, K.; Huber, R.; Michel, H. *J. Mol. Biol.* **1984**, *180*, 385.

(7) Trebst, A. *Z. Naturforsch.* **1985**, *41*, 240.
(8) Seibert, M. In *The Photosynthetic Reaction Center;* Deisenhofer, J., Norris, J., Eds.; Academic Press: San Diego, CA, 1993; Vol. I, p 319.
(9) Renger, T.; Marcus, R. A. *J. Phys. Chem. B* **2002**, *106*, 1809.
(10) Jankowiak, R.; Hayes, J. M.; Small, G. J. *J. Phys. Chem.* B **2002**, *106*, 8803.
(11) Kwa, S. L. S.; Eijckelhoff, C.; van Grondelle, R.; Dekker, J. P. *J. Phys. Chem.* **1994**, *98*, 7702.
(12) Fromme, P. Private communication.
(13) Small, G. J. *Chem. Phys.* **1995**, *197*, 239.
(14) Vacha, F.; Joseph, D. M.; Durrant, J. R.; Telfer, A.; Klug, D. R.; Porter, G.; Barber, J. *Proc. Natl. Acad. Sci. U.S.A.* **1995**, *92*, 2929.
(15) Johnson, S. G.; Tang, D.; Jankowiak, R.; Hayes, J. M.; Small, G. J. *J. Phys. Chem.* **1989**, *93*, 5953.
(16) Durrant, J. R.; Klug, D. R.; Kwa, S. L. S.; van Grondelle, R.; Porter, G.; Dekker, J. P. *Proc. Natl. Acad. Sci. U.S.A.* **1995**, *92*, 4798.
(17) These calculations assumed, in part, that the $P_1-P_2$ distance is 10 Å.
(18) Reducing the $P_1-P_2$ distance from 10 to 8.6 Å may result in more localization of P680* on $P_1$ and $P_2$. At the time of this writing, the coordinates of the refined structure had not been released.
(19) Prokhorenko, V. I.; Holzwarth, A. R. *J. Phys. Chem. B* **2000**, *104*, 11563.
(20) Dahlbom, M.; Pullerits, T.; Mukamel, S.; Sundström, V. *J. Phys. Chem. B* **2001**, *105*, 5515.
(21) Meier, T.; Chernak, V.; Mukamel, S. *J. Phys. Chem. B* **1997**, *101*, 7332.
(22) Wasielewski, M. R.; Johnson, D. G.; Seibert, M.; Govindjee. *Proc. Natl. Acad. Sci. U.S.A.* **1989**, *86*, 524.
(23) Wiederrecht, G. P.; Seibert, M.; Govindjee; Wasielewski, M. R. *Proc. Natl. Acad. Sci. U.S.A.* **1994**, *91*, 8999.
(24) Schelvis, J. P. M.; van Noort, P. I.; Aartsma, T. J.; van Gorkom, H. J. *Biochim. Biophys. Acta* **1994**, *1184*, 242.
(25) Gatzen, G.; Müller, M. G.; Griebenow, K.; Holzwarth, A. R. *J. Phys. Chem.* **1996**, *100*, 7269.
(26) Greenfield, S. R.; Seibert, M.; Govindjee; Wasielewski, M. R. *J. Phys. Chem. B* **1997**, *101*, 2251.
(27) Merry, S. A.; Kumazaki, S.; Tachibana, Y.; Joseph, D. M.; Porter, G.; Yoshihara, K.; Barber, J.; Durrant, J. R.; Klug, D. R. *J. Phys. Chem.* **1996**, *100*, 10469.
(28) Groot, M.-L.; van Mourik, F.; Eijckelhoff, C.; van Stokkum, I. H. M.; Dekker, J.; van Grondelle, R. *Proc. Natl. Acad. Sci. U.S.A.* **1997**, *94*, 4389.
(29) Jankowiak, R.; Tang, D.; Small, G. J.; Seibert, M. *J. Phys. Chem.* **1989**, *93*, 1649.
(30) Tang, D.; Jankowiak, R.; Seibert, M.; Small, G. J. *Photosynth. Res.* **1991**, *27*, 19.
(31) Wasielewski, M. R.; Johnson, D.; Gorindjee; Preston, C.; Seibert, M.; *Photosynth. Res.* **1989**, *22*, 89.
(32) Visser, H. M.; Groot, M.-L.; van Mourik, F.; van Stokkum, I. H.; Dekker, J. P.; van Grondelle, R. *J. Phys. Chem.* **1995**, *99*, 15304.
(33) Greenfield, S. R.; Seibert, M.; Wasielewski, M. R. *J. Phys. Chem. B* **1999**, *103*, 8364.
(34) Leegwater, J. A.; Durrant, J. R.; Klug, D. R. *J. Phys. Chem. B* **1997**, *101*, 7205.
(35) Vink, K. J.; de Boer, S.; Plijter, J. J.; Hoff, A. J.; Wiersma, D. A. *Chem. Phys. Lett.* **1987**, *142*, 433.
(36) Völker, S. *J. Lumin.* **1987**, *36*, 251.
(37) van der Zaag, P. J.; Galaup, J. P.; Völker, S. *Chem. Phys. Lett.* **1990**, *174*, 467.
(38) Hayes, J. M.; Lyle, P. A.; Small, G. J. *J. Phys. Chem.* **1994**, *98*, 7337.
(39) Berthold, D. A.; Babcock, G. T.; Yocum, C. F. *FEBS Lett.* **1981**, *134*, 231.
(40) Eijckelhoff, C.; Dekker, J. P. *Photosynth. Res.* **1997**, *52*, 69.
(41) den Hartog, E. T. H.; Vacha, F.; Lock, A. J.; Barber, J.; Dekker, J. P.; Völker, S. *J. Phys. Chem. B* **1998**, *102*, 9174.
(42) Jankowiak, R.; Rätsep, M.; Picorel, R.; Seibert, M.; Small, G. J. *J. Phys. Chem. B* **1999**, *103*, 9759.
(43) Tetenkin, V. L.; Gulyaev, B. A.; Seibert, M.; Rubin, A. B. *FEBS Lett.* **1989**, *250*, 459.
(44) Tang, D.; Jankowiak, R.; Seibert, M.; Yocum, C. F.; Small, G. J. *J. Phys. Chem.* **1990**, *94*, 6519.
(45) Breton, J. In *Perspectives in Photosynthesis;* Jortner, J., Pullman, B., Eds.; Kluwer Academic Publishers: Dordrecht, The Netherlands, 1989; pp 23−38.
(46) Reddy, N. R. S.; Picorel, R.; Small, G. J. *J. Phys. Chem.* **1992**, *96*, 6458.
(47) Tang, D.; Jankowiak, R.; Seibert, M.; Small, G. J. *Photosynth. Res.* **1991**, *27*, 19.
(48) Chang, H.-C.; Jankowiak, R.; Yocum, C. F.; Picorel, R.; Alfonso, M.; Seibert, M.; Small, G. J. *J. Phys. Chem.* **1994**, *98*, 7717.
(49) Reinot, T.; Small, G. J. *J. Chem. Phys.* **2001**, *114*, 9105.
(50) Dang, N.; Reinot, T.; Small, G. J. To be submitted to *J. Chem. Phys.* for publication.
(51) Lyle, P. A.; Kolaczkowski, S. V.; Small, G. J. *J. Phys. Chem.* **1993**, *97*, 6926.
(52) Zazubovich, V.; Matsuzaki, S.; Johnson, T. W.; Hayes, J. M.; Chitnis, P. R.; Small, G. J. *Chem. Phys.* **2002**, *275*, 47.
(53) Hayes, J. M.; Matsuzaki, S.; Rätsep, M.; Small, G. J. *J. Phys. Chem. B* **2000**, *104*, 836.
(54) Shu, L.; Small, G. J. *J. Opt. Soc. Am. B* **1992**, *9*, 738.
(55) Kim, W.-H.; Reinot, T.; Hayes, J. M.; Small, G. J. *J. Phys. Chem.* **1995**, *99*, 7300.
(56) Reinot, T.; Zazubovich, V.; Hayes, J. M.; Small, G. J. *J. Phys. Chem. B* **2001**, *105*, 5083.
(57) Chang, H.-C.; Small, G. J.; Jankowiak, R. *Chem. Phys.* **1995**, *194*, 323.